

Spherical cellulose gel particles with donut-shaped interior structures

Goeun Sim · Theo G. M. van de Ven

Received: 12 November 2014 / Accepted: 20 January 2015 / Published online: 28 January 2015
© Springer Science+Business Media Dordrecht 2015

Abstract Partially carboxylated cellulose wood fibers (CMF) with highly swollen balloon-like structures were ultrasonicated to produce spherical cellulose gel particles with donut-shaped interior structure. The formation of these particles is most likely due to the characteristic microfibril arrangements in swollen CMF consisting of alternating regions of “balloons” and “collars”, which have different structural rigidity. Upon applying an intense mechanical energy, the more physically strained parts break up prior to the flexible areas. Hence the helically extended S1 microfibrils and the axially compressed S3 layers are damaged first, while partially or fully carboxymethylated flexible cellulose chains in the S2 layers are rearranging themselves around the tightly wound collars. The interior donut structure likely originates from the collars, which do not collapse upon drying. The carboxymethylated spherical cellulose gel particles have a wide size distributions ranging from 15 to 200 μm in diameter with excellent rewettability and pH sensitivity in water.

Keywords Cellulose gel particles · Carboxymethylated wood fibers · Wood fiber structures · Break-up of cellulose wood fibers

Introduction

Utilizing cellulose based materials often requires substantial amounts of chemical and mechanical treatments. In preparation of cellulose nanomaterials, carboxylation is often used to facilitate the fibrillation process by introducing electrostatic repulsion and disrupting interfibrillar hydrogen bonding (Eyholzer et al. 2009; Siró and Plackett 2010; Isogai et al. 2011; Klemm et al. 2011; Liimatainen and Visanko 2012). With increased amounts of carboxyl groups available on the fiber surface, the fiber becomes more and more swollen until the structures are completely disintegrated (Rácz and Borsa 1997; Saito et al. 2007; Sim et al. 2014). Microfibrils in the secondary wood cell wall undergo structural changes, which vary depending on the type of pulp used and the chemistry applied. Understanding the deformed fiber structures is critical as they relate to some of the important issues in cellulose chemistry such as non-uniform fiber fragmentation and low reaction yield.

Balloon-like swollen fiber structures have been reported during carboxymethylation, quaternization, fiber dissolution in several solvents, and high pressure homogenization (Jardeby et al. 2005a; Cuissinat and Navard 2006; Iwamoto et al. 2007; Le Moigne et al. 2008, 2010a; Pei et al. 2013; Uetani and Yano 2011). Carboxymethylation is widely used in many fields of applications as it forms pH responsive hydrocolloid microgel particles with increased water absorbency and viscosity (Rathna et al. 1996; Chen and Fan 2008) while providing potential reaction sites which enables further

G. Sim · T. G. M. van de Ven (✉)
Department of Chemistry, Pulp and Paper Research
Centre, Centre for Self-Assembled Chemical Structures,
McGill University, Montreal, QC, Canada
e-mail: theo.vandeven@mcgill.ca

tailoring (Khullar et al. 2005; Jiang et al. 2009; Qi et al. 2010; Pelton and Hoare 2011; Bocek et al. 2011; Dhar et al. 2012). Figure 1 shows the characteristic features of carboxymethylated fibers (CMF) such as: (1) extended S1 microfibrils helically winding the exterior of the balloons, (2) tightly wound S1 microfibrils creating collars, (3) S2 microfibrils filling up the balloons, (4) innermost S3 layer with high microfibril angles (MFA).

In previous work, we found that CMF exceeding 1.5 mmol/g charge groups show balloon-like structures, which is caused by the microfibril arrangements in S1, S2, and S3 layers in wood cell walls (Sim et al. 2014). While attempting to isolate the S3 layers from the balloons, we have learnt that the shapes of CMF fragments vary largely depending on the types and amount of energy applied to the CMF suspensions (Sim and van de Ven 2015). Applying ultrasonication damages CMF and produces “spherical particles” that are distinguishably different from the highly swollen “flat rings” that were reported in other studies (Jardeby et al. 2004, 2005a, 2005b; Cuissinat and Navard 2006; Le Moigne et al. 2010a). Based on microscopic observations, we propose a break-up mechanism of CMF subjected to intense mechanical energy, which leads to the formation of spherical cellulose gel particles with donut-shaped interior structures. At the same time, studying the break-up of the balloons will provide additional information about their interior structure.

Experimental

Materials

Bleached softwood kraft fiber sheets (SKF; Domtar, Canada) were used as a starting material. Reagent grade

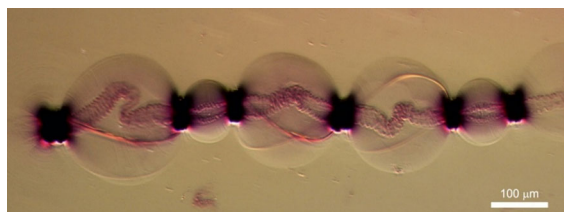


Fig. 1 Hoffman modulation contrast microscopy of toluidine blue dyed carboxymethylated kraft, bleached softwood fiber (CMF) with 2.35 mmol/g of carboxylate contents. Image was taken prior to applying any mechanical treatments

sodium chloroacetate (MCA), sodium hydroxide (NaOH), hydrochloric acid (HCl), *N*-(3-Dimethylaminopropyl)-*N'*-ethylcarbodiimide hydrochloride (EDC), and 5-aminofluorescein (A-fluo) were purchased from Sigma-Aldrich and were used as received.

Preparation of carboxymethylated fibers (CMF) and CMF gel

Softwood kraft fibers were carboxymethylated and fluorescently tagged following the method reported by Sim et al. (2014). The carboxyl contents of CMF were measured by conductometric titration (Metrohm 836 Titrando), according to Yang et al. (2012). Both fluorescently tagged and untagged carboxymethylated fiber suspensions (CMF, 0.1 % w/w) were ultrasonicated (Hielscher, UP200H; 200 W, 24 kHz) for 1 min to produce gel particles. To study intermediate structures, another CMF suspension was placed in the ultrasonic cleaning bath (Branson, B200; 19 W, 50/60 Hz) for 1 min. Samples were drawn every 10 s for microscopic observations.

Microscopic observations

Ultrasonicated, untagged CMF gel suspensions were dyed with toluidine blue and observed by Hoffman modulation contrast microscopy (HMC, Nikon Eclipse TE2000-U). The sample slides were air dried overnight at room temperature and re-wetted by adding a drop of water between the slide and the coverslip.

For confocal laser scanning microscopy (CLSM), A-fluo treated CMF gel suspensions were excited at $\lambda = 494$ nm with an exposure time of 800 ms (Zeiss LSM510; 488 nm, Ar laser, 30 mW). Each coverslip was sealed with two spacers (0.24 mm in total thickness) to minimize gel deformation. All confocal imaging was done in water immersion to minimize refraction.

An aqueous suspension of gel particles was deposited on a mica surface, air-dried, and then sputter-coated with platinum with a thickness of 10 nm. Images were made with a high resolution field emission scanning electron microscope (FE-SEM; FEI Inspect, F-50) which was operated at an accelerating voltage of 5.0 kV to observe the surface morphology of the dried gel particles.

Results and discussion

Carboxymethylated fibers (CMF) with 2.35 mmol/g of COO groups are highly swollen and form balloon-like structures in water at neutral pH. The degree of “ballooning” mainly depends on the number of charged groups that are introduced by carboxymethylation. When carrying 2–2.5 mmol of charged groups, the ballooning effect is the most prominent whereas CMF with below 2.0 mmol of COO groups often have various ranges of non-swollen areas. Roughly above 3.0 mmol, the CMF disintegrates and dissolves in water as carboxymethylated cellulose (CMC) (Tejado et al. 2012). When an ultrasonication is applied to the CMF suspension for several tens of seconds, the fibers break into small fragments that are predominantly spherical. Sizes of the spherical particles vary from 15 to 200 μm in diameter as can be seen in Fig. 2. Toluidine blue is an ion exchange dye which can access the negatively charged groups in the pores of cellulose fibers (van de Ven et al. 2007). In Hoffman modulation light microscopy, all samples were dyed with toluidine blue at least 30 min prior to imaging for a better contrast. Within the spherical gel particles, the interior donut-shaped structures appear to be more heavily dyed than the balloon areas (Fig. 2a, b), suggesting that the negatively charged cellulose chains are more densely packed in the donuts. The donuts are most probably originated from the “collars” in CMF, where microfibrils in all S1, S2, and S3 layers are deposited upon ballooning (Sim et al. 2014). This is in agreement with the confocal laser scanning microscopic (CLSM) observations, in which the COO groups in donut areas show stronger fluorescent intensity (Fig. 2c). When CLSM scans were reconstructed in 3D, a sphere was observed as presented in Fig. 2d. Studies have shown that during the fiber swelling and fragmentation in prolonged chemical treatments, the fiber breaks down into “flat rings” rather than spheres (Jardeby et al. 2004; Le Moigne and Navard 2009; Le Moigne et al. 2010b). The break-up mechanism of the swollen fibers, CMF in this case, by applying ultrasonication is obviously different from that by increasing the chemical treatment time.

In order to monitor intermediate structures of the CMF during mechanical break-up, a CMF suspension placed in an ultrasonic cleaning bath was

microscopically observed. It appears that the helically wound S1 microfibrils are restricting the swollen fiber mobility during ultrasonication. This results a severe axial distortion and yields a structure shown in Fig. 3a. As a consequence, an increased amount of tension is build up on the helices and it eventually reaches the point where they fracture (3b). Same principle applies to the S3 layers that are already under axial compression, hence they are cleaved before the balloons break open (3c).

Based on microscopic observations made in Figs. 2 and 3, we propose a break-up mechanism in Fig. 4. When a highly swollen CMF suspension is ultrasonicated (4a), the balloons break apart (4b). The balloon break-up is associated with the damaged S1 microfibrils that are helically extended around the balloons, as well as the cleavage of the axially compressed S3 layers. Within the fiber fragments (4c), the S2 microfibrils rearrange to form spheres as shown in 4d. During this process, the S3 layers can be separated out and suspended in solution. The most remarkable transformation in our proposed mechanism is from Fig. 4c, d. This transition was not directly observed microscopically, conceivably because of the fast rearrangement of the S2 fibrils around the collars after the balloon break-up.

The rewettability of the spherical gel particles was qualitatively analyzed by going through two drying cycles (Fig. 5). After imaging 5a, the slide was left overnight in an ambient condition without removing the coverslip. Upon drying, thin branches that are rooted at the collars were formed to make globular structures as seen in 5b. The formation of the branched structures is most probably a drying effect which occurs when the cellulosic materials held together inside the balloons—unmodified, partially and fully carboxymethylated cellulose chains—are dried together. As the dried samples were rewetted by adding a drop of water between the coverslip and the slide, the flattened sphere reformed to its swollen state in a few seconds, 5c. When the rewetted sample was dried again in the same manner as before, the thin branches were regenerated but they do not come together in same shape as before, 5d. The fact that the sphere in 5c is only slightly smaller diameter as in 5a suggests that these gel particles have a good rewettability.

The surface morphology of dried gel particles was observed by SEM. Thin branches seen in Fig. 5b, d were not observed in this case probably because of the

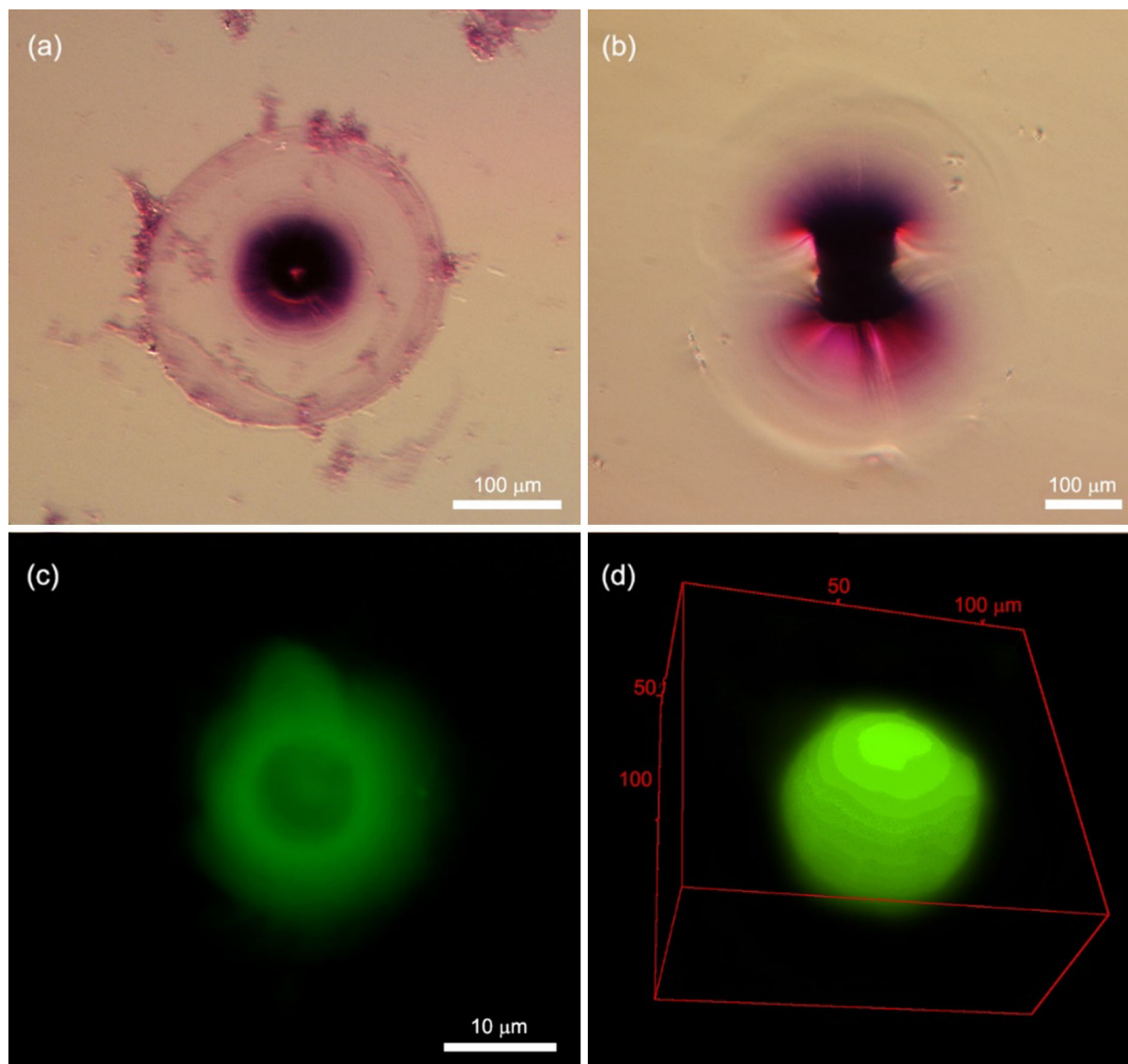


Fig. 2 Spherical gel particles of various sizes. Toluidine blue dyed spherical gel particles observed by Hoffman modulation microscopy (**a**, **b**). A z-stacked confocal laser scanning

microscopic (CLSM) image a fluorescently tagged particle (**c**). A 3D image of the sphere from CLSM scans is shown in (**d**)

differences in surface energy of the two substrates, glass (Fig. 5) and mica (Fig. 6). Relatively rougher glass surface provides more anchoring sites than a smooth mica surface, thereby promoting cellulose chain aggregation that leads to the formation of branched structures. When the spherical particles were dried on a mica, the spheres are collapsed upon the collars, creating the interior donut-shaped structures. The dried donuts appear to be composed of approximately 1–2 μm thick spirals, where the

literature reported thickness of the S1 layer in native softwood fibers is about 0.1–0.2 μm (Booker and Sell 1998). This may indicate that the collars are mainly composed of S1 microfibrils and that the flexible S2 cellulose fibrils held inside the balloons are collapsed on this interior skeleton. As a consequence, an apparent thickness of each spiral is increased by 5–10 times.

Due to the heterogeneous nature of the wood fiber structures, the chemically modified fibers often show

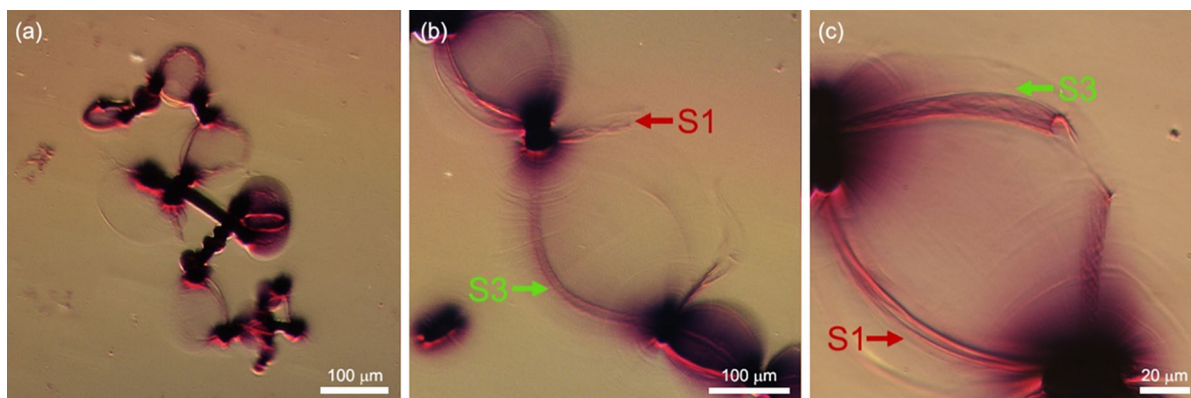


Fig. 3 Fiber fragments in CMF suspension left inside the ultrasonic cleaning bath for 1 min. CMF experiences axial distortion (a), followed by S1 (b) and S3 layer break-up (c). S1 and S3 break-ups are not sequential

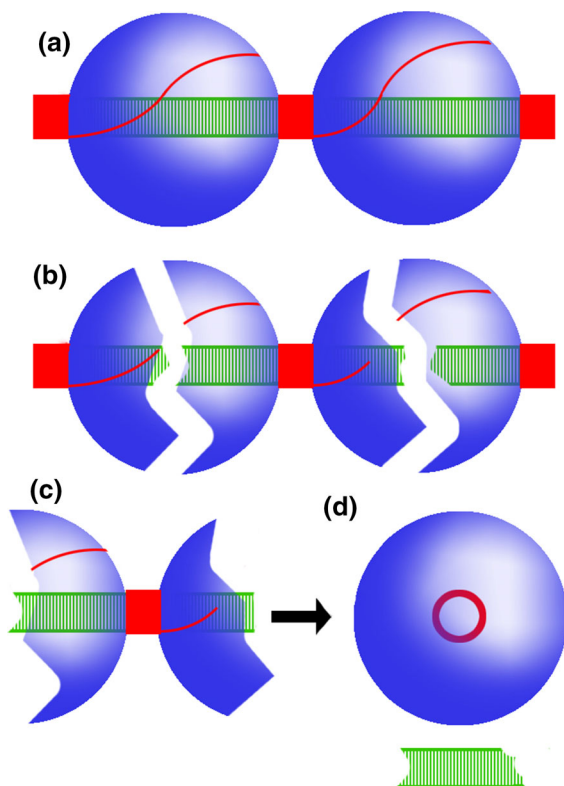


Fig. 4 Proposed break-up mechanism of CMF by applying ultrasonication. Microfibrils in each secondary layer are color coded, S1 in red, S2 in blue, and S3 in green. A highly swollen, balloon-like structure before applying any mechanical treatments (a). Ultrasonication damages microfibrils in the balloon area and CMF starts to fragment (b). The fragment (c) rearranges into a sphere and the S3 layer is often separated from the sphere (d). All drawings are approximately to scale

various shapes and a wide size distributions. Examples of non-spherical structures are shown in Fig. 7. Chopped off CMF with more than two spheres are often seen, along with isolated S3 layers that are partially damaged or shortened (7a). Fluorescent tagged non-spherical particles show that the donut-shaped interior structure maintains the characteristic features of S1 collars, where the charged cellulose chains are highly concentrated while forming tightly wound spirals (7b). The surface tagged S3 layers sometimes remain inside the spherical gel particles. Figure 7c shows a S1 microfibril protruding from the donut-shaped spirals, whereas Fig. 6 showed closed, thick donuts with an empty space in the middle.

Figure 8 shows a spherical gel particle before (a) and after (b) adding a drop of 1 M HCl solution. As the free carboxyl groups are protonated, the gel boundary becomes more defined and the overall diameter decreases. Although there are no significant changes in the interior donut-shaped structure, they appear slightly thicker after the addition of acid.

Concluding remarks

Efforts have been made to optimize cellulose processing by improving the cellulose fiber dissolution, which is unfavourable in many solvent systems including water. Heterogeneous swelling of the fibers, thereby creating balloon-like structures, is often seen while chemically processing the fibers. The fact that the

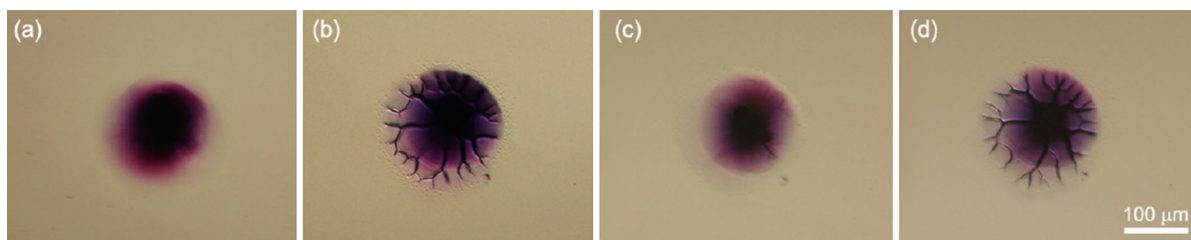


Fig. 5 HMC of gel suspended in water (a), air-dried overnight at room temperature (b), rewetted by adding a drop of water (c), and then re-dried under the same condition as b (d)

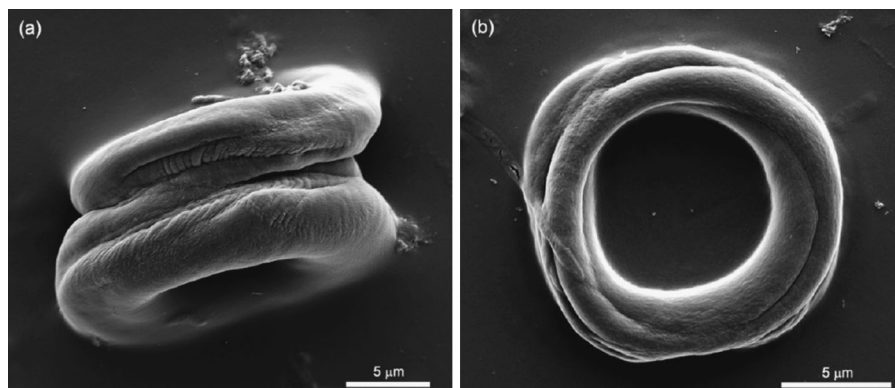


Fig. 6 SEM of gel particles deposited on mica, air-dried overnight. All samples are Pt coated (10 nm). Thick donut-shaped structures that are composed of tight spirals are observed from the side (a); and from the top (b)

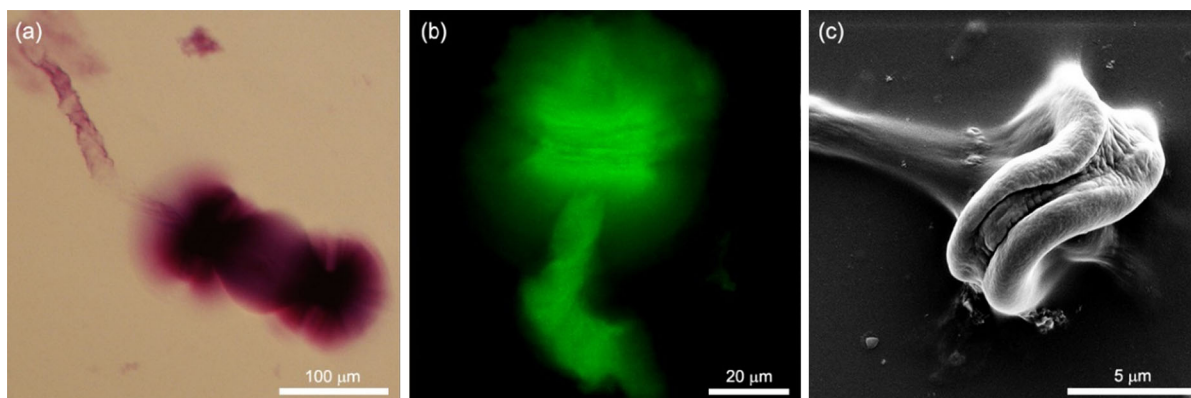


Fig. 7 Non-spherical structures produced by ultrasonication of the CMF suspension. HMC of a series of spheres in a shortened CMF and an isolated S3 layer (a); CLSM of a sphere with

protruding S3 layers (b); and SEM of dried non-spherical particle on a mica surface with a protruding S1 microfibrils (c)

ballooning occurs in both aqueous and non-aqueous solvent systems and during carboxylating chemistries indicates that this phenomenon is mainly related to the cellulose microfibril arrangements in fiber wall. The underlying findings of this work illustrate the

structural evolution of partially carboxylated cellulose fibers while going through a subsequent mechanical treatment. Our proposed break-up mechanism based on microscopic observations suggest that the altered microfibril arrangements occurring at the swelling

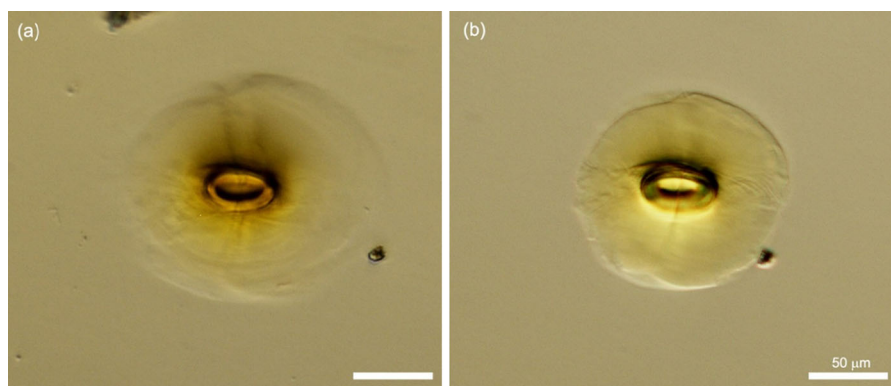


Fig. 8 HMC of A-fluo tagged gel in water at neutral pH (a) and after adding a drop of 1 M HCl (b)

stage create areas of different structural rigidity, which prevents a complete fiber dissolution. The produced spherical gel particles with interior donut-shaped structure may have applications in drug delivery or sensing, where micrometer sized gel particles with rewettability and pH responsibility are required.

Acknowledgments This work was supported by an NSERC Industrial Research Chair, supported by FPInnovations, by the NSERC Green Fibre Network, and by the FQRNT Centre for Self-Assembled Chemical Structures. Special thanks to McGill Cell Imaging and Analysis Network and McGill Facility for Electron Microscopy Research.

References

- Bochek AM, Zabivalova NM, Yudin VE et al (2011) Properties of carboxymethyl cellulose aqueous solutions with nanoparticle additives and the related composite films. *Polym Sci Ser A* 53:1167–1174. doi:[10.1134/S0965545X11120029](https://doi.org/10.1134/S0965545X11120029)
- Booker RE, Sell J (1998) The nanostructure of the cell wall of softwoods and its functions in a living tree. *Holz als Roh- und Werkstoff* 56(1):1–8. doi:[10.1007/s001070050255](https://doi.org/10.1007/s001070050255)
- Chen H, Fan M (2008) Novel thermally sensitive pH-dependent chitosan/carboxymethyl cellulose hydrogels. *J Bioact Compat Polym* 23:38–48. doi:[10.1177/0883911507085070](https://doi.org/10.1177/0883911507085070)
- Cuissinat C, Navard P (2006) Swelling and dissolution of cellulose part 1: free floating cotton and wood fibres in N-Methylmorpholine-N-oxide–water mixtures. *Macromol Symp* 244:1–18. doi:[10.1002/masy.200651201](https://doi.org/10.1002/masy.200651201)
- Dhar N, Akhlaghi SP, Tam KC (2012) Biodegradable and biocompatible polyampholyte microgels derived from chitosan, carboxymethyl cellulose and modified methyl cellulose. *Carbohydr Polym* 87:101–109. doi:[10.1016/j.carbpol.2011.07.022](https://doi.org/10.1016/j.carbpol.2011.07.022)
- Eyholzer C, Bordeanu N, Lopez-Suevos F et al (2009) Preparation and characterization of water-redispersible nanofibrillated cellulose in powder form. *Cellulose* 17:19–30. doi:[10.1007/s10570-009-9372-3](https://doi.org/10.1007/s10570-009-9372-3)
- Isogai A, Saito T, Fukuzumi H (2011) TEMPO-oxidized cellulose nanofibers. *Nanoscale* 3:71–85. doi:[10.1039/c0nr00583e](https://doi.org/10.1039/c0nr00583e)
- Iwamoto S, Nakagaito AN, Yano H (2007) Nano-fibrillation of pulp fibers for the processing of transparent nanocomposites. *Appl Phys A* 89:461–466. doi:[10.1007/s00339-007-4175-6](https://doi.org/10.1007/s00339-007-4175-6)
- Jardebey K, Lennholm H, Germgård U (2004) Characterisation of the undissolved residuals in CMC-solutions. *Cellulose* 11:195–202
- Jardebey K, Germgård U, Kreutz B et al (2005a) The influence of fibre wall thickness on the undissolved residuals in CMC solutions. *Cellulose* 12:167–175. doi:[10.1007/s10570-004-1371-9](https://doi.org/10.1007/s10570-004-1371-9)
- Jardebey K, Germgård U, Kreutz B et al (2005b) Effect of pulp composition on the characteristics of residuals in CMC made from such pulps. *Cellulose* 12:385–393. doi:[10.1007/s10570-005-2202-3](https://doi.org/10.1007/s10570-005-2202-3)
- Jiang L, Li Y, Zhang L, Wang X (2009) Preparation and characterization of a novel composite containing carboxymethyl cellulose used for bone repair. *Mater Sci Eng C* 29:193–198. doi:[10.1016/j.msec.2008.06.009](https://doi.org/10.1016/j.msec.2008.06.009)
- Khullar R, Varshney VK, Naithani S et al (2005) Carboxymethylation of cellulosic material (average degree of polymerization 2600) isolated from cotton (*Gossypium*) linters with respect to degree of substitution and rheological behavior. *J Appl Polym Sci* 96:1477–1482. doi:[10.1002/app.21645](https://doi.org/10.1002/app.21645)
- Klemm D, Kramer F, Moritz S et al (2011) Nanocelluloses: a new family of nature-based materials. *Angew Chem Int Ed Engl* 50:5438–5466. doi:[10.1002/anie.201001273](https://doi.org/10.1002/anie.201001273)
- Le Moigne N, Navard P (2009) Dissolution mechanisms of wood cellulose fibres in NaOH–water. *Cellulose* 17:31–45. doi:[10.1007/s10570-009-9370-5](https://doi.org/10.1007/s10570-009-9370-5)
- Le Moigne N, Montes E, Pannetier C et al (2008) Gradient in dissolution capacity of successively deposited cell wall layers in cotton fibres. *Macromol Symp* 262:65–71. doi:[10.1002/masy.200850207](https://doi.org/10.1002/masy.200850207)
- Le Moigne N, Bikard J, Navard P (2010a) Rotation and contraction of native and regenerated cellulose fibers upon

- swelling and dissolution: the role of morphological and stress unbalances. *Cellulose* 17:507–519. doi:[10.1007/s10570-009-9395-9](https://doi.org/10.1007/s10570-009-9395-9)
- Le Moigne N, Jardeby K, Navard P (2010b) Structural changes and alkaline solubility of wood cellulose fibers after enzymatic peeling treatment. *Carbohydr Polym* 79:325–332. doi:[10.1016/j.carbpol.2009.08.009](https://doi.org/10.1016/j.carbpol.2009.08.009)
- Liimatainen H, Visanko M (2012) Enhancement of the nanofibrillation of wood cellulose through sequential periodate–chlorite oxidation. *Biomacromolecules* 13:1592–1597
- Pei A, Butchosa N, Berglund LA, Zhou Q (2013) Surface quaternized cellulose nanofibrils with high water absorbency and adsorption capacity for anionic dyes. *Soft Matter* 9:2047. doi:[10.1039/c2sm27344f](https://doi.org/10.1039/c2sm27344f)
- Pelton R, Hoare T (2011) Microgels and their synthesis: an introduction. In: *Microgel suspensions: fundamentals and applications*. Wiley-VCH Verlag GmbH & Co. KGaA, Weinheim, Germany, pp 1–32. doi:[10.1002/9783527632992.ch1](https://doi.org/10.1002/9783527632992.ch1)
- Qi H, Liebert T, Meister F et al (2010) Homogenous carboxymethylation of cellulose in the new alkaline solvent LiOH/urea aqueous solution. *Macromol Symp* 294:125–132. doi:[10.1002/masy.200900166](https://doi.org/10.1002/masy.200900166)
- RÁCZ I, Borsá J (1997) Swelling of carboxymethylated cellulose fibres. *Cellulose* 4:293–303
- Rathna GVN, Mohan Rao DV, Chatterji PR (1996) Hydrogels of gelatin-sodium carboxymethyl cellulose: synthesis and swelling kinetics. *J Macromol Sci Part A* 33:1199–1207. doi:[10.1080/10601329608010914](https://doi.org/10.1080/10601329608010914)
- Saito T, Kimura S, Nishiyama Y, Isogai A (2007) Cellulose nanofibers prepared by TEMPO-mediated oxidation of native cellulose. *Biomacromolecules* 8:2485–2491. doi:[10.1021/bm0703970](https://doi.org/10.1021/bm0703970)
- Sim G, van de Ven TGM (2015) The S3 layer isolated from carboxymethylated cellulose wood fibers. *Cellulose* 22(1):45–52. doi:[10.1007/s10570-014-0503-0](https://doi.org/10.1007/s10570-014-0503-0)
- Sim G, Alam M, Godbout L, van de Ven TGM (2014) Structure of swollen carboxylated cellulose fibers. *Cellulose* 21:4595–4606. doi:[10.1007/s10570-014-0425-x](https://doi.org/10.1007/s10570-014-0425-x)
- Siró I, Plackett D (2010) Microfibrillated cellulose and new nanocomposite materials: a review. *Cellulose* 17:459–494. doi:[10.1007/s10570-010-9405-y](https://doi.org/10.1007/s10570-010-9405-y)
- Tejado A, Alam MN, Antal M et al (2012) Energy requirements for the disintegration of cellulose fibers into cellulose nanofibers. *Cellulose* 19:831–842. doi:[10.1007/s10570-012-9694-4](https://doi.org/10.1007/s10570-012-9694-4)
- Uetani K, Yano H (2011) Nanofibrillation of wood pulp using a high-speed blender. *Biomacromolecules* 12:348–353. doi:[10.1021/bm101103p](https://doi.org/10.1021/bm101103p)
- Van de Ven TGM, Saint-Cyr K, Allix M (2007) Adsorption of toluidine blue on pulp fibers. *Colloids Surf A Physicochem Eng Asp* 294:1–7. doi:[10.1016/j.colsurfa.2006.07.040](https://doi.org/10.1016/j.colsurfa.2006.07.040)
- Yang H, Tejado A, Alam N et al (2012) Films prepared from electrosterically stabilized nanocrystalline cellulose. *Langmuir* 28:7834–7842. doi:[10.1021/la2049663](https://doi.org/10.1021/la2049663)